

This work was written as part of one of the author's official duties as an Employee of the United States Government and is therefore a work of the United States Government. In accordance with 17 U.S.C. 105, no copyright protection is available for such works under U.S. Law.

Public Domain Mark 1.0

<https://creativecommons.org/publicdomain/mark/1.0/>

Access to this work was provided by the University of Maryland, Baltimore County (UMBC) ScholarWorks@UMBC digital repository on the Maryland Shared Open Access (MD-SOAR) platform.

Please provide feedback

Please support the ScholarWorks@UMBC repository by emailing scholarworks-group@umbc.edu and telling us what having access to this work means to you and why it's important to you. Thank you.

Background and pickup ion velocity distribution dynamics in Titan's plasma environment: 3D hybrid simulation and comparison with CAPS T9 observations

A.S. Lipatov^{a,*}, E.C. Sittler Jr.^b, R.E. Hartle^b, J.F. Cooper^b, D.G. Simpson^b

^a *GPHI UMBC/NASA GSFC, Code 673, Greenbelt, MD 20771, USA*

^b *NASA Goddard Space Flight Center, Greenbelt, MD 20771, USA*

Received 24 September 2010; received in revised form 12 May 2011; accepted 23 May 2011

Available online 30 May 2011

Abstract

In this report we discuss the ion velocity distribution dynamics from the 3D hybrid simulation. In our model the background, pickup, and ionospheric ions are considered as particles, whereas the electrons are described as a fluid. Inhomogeneous photoionization, electron-impact ionization and charge exchange are included in our model. We also take into account the collisions between the ions and neutrals. The current simulation shows that mass loading by pickup ions H^+ , H_2^+ , CH_4^+ and N_2^+ is stronger than in the previous simulations when O^+ ions are introduced into the background plasma. In our hybrid simulations we use Chamberlain profiles for the atmospheric components. We also include a simple ionosphere model with average mass $M = 28$ amu ions that were generated inside the ionosphere. The moon is considered as a weakly conducting body. Special attention will be paid to comparing the simulated pickup ion velocity distribution with CAPS T9 observations. Our simulation shows an asymmetry of the ion density distribution and the magnetic field, including the formation of the Alfvén wing-like structures. The simulation also shows that the ring-like velocity distribution for pickup ions relaxes to a Maxwellian core and a shell-like halo.

© 2011 COSPAR. Published by Elsevier Ltd. All rights reserved.

Keywords: Ionospheres; Atmospheres; Induced magnetospheres; Magnetic barrier; Alfvén wing; Satellites

1. Introduction

Wave-particle interactions play a very important role in plasma dynamics near Titan: mass loading, excitation of low-frequency waves and the formation of the particle velocity distribution function (e.g. ring/shell-like distributions, etc.) The kinetic approach is important for the

estimation of collision processes (e.g. a charge exchange). Particle-wave interactions play a very important role in the possible formation of a shock wave or an Alfvén wing, and in coupling of pickup ions and background ions via excitation of low-frequency waves. These kinetic processes become important in the formation of an obstacle for the background plasma.

Magnetohydrodynamic (MHD) simulations have been useful for the study of the interaction between plasma flow and Titan (Keller and Cravens, 1994; Ledvina and Cravens, 1998; Cravens et al., 1998; Kabin et al., 1999, 2000; Nagy et al., 2001). MHD simulations demonstrated a global picture of magnetospheric interaction with a moon, including mass loading the magnetosphere's plasma with the atmosphere's pickup ions and possible chemical

* Corresponding author. Address: NASA GSFC, Code 673, Bld. 21, Rm. 247, 8800 Greenbelt Rd., Greenbelt, MD 20771, USA. Tel.: +1 3012860906.

E-mail addresses: Alexander.Lipatov-1@nasa.gov (A.S. Lipatov), Edward.C.Sittler@nasa.gov (E.C. Sittler Jr.), Richard.E.Hartle@nasa.gov (R.E. Hartle), John.F.Cooper@nasa.gov (J.F. Cooper), David.G.Simpson@nasa.gov (D.G. Simpson).

processes inside the exobase where the fluid approximation is good enough. However, several kinetic effects have been lost, namely: asymmetry in the form of an Alfvén wing and a magnetic barrier near a moon, an asymmetry in the atmosphere’s pickup ion distribution, possible plasma structure with a thickness of the order of the heavy ion gyroradius, an overestimate of the pickup ion fluxes along the magnetic field, and the absence of kinetic effects inside plasma structures. Many of these effects may be recovered by using hybrid simulations.

Several 3D hybrid simulations of Titan plasma interactions were performed during the last decade as described in papers by Brecht et al. (2000), Kallio et al. (2004), Sillanpää et al. (2006), Modolo et al. (2007a), Simon et al. (2007), Kallio et al. (2007), Modolo and Chanteur (2008). These simulations were devoted to an interpretation of Voyager 1 and Cassini data and assumed the presence of the heavy ions like O^+ in magnetospheric plasma. Kallio et al. (2007), discusses hybrid modeling for the T9 case in the presence of H_2^+ and H_1^+ ions in the background plasma. However, they used a higher total density (0.4 cm^{-3}) for these ions than was observed in the CAPS T9 measurements (0.05 cm^{-3}) (Sittler et al., 2010). The main results that were obtained in these hybrid simulations are the following: asymmetry of a nonstationary bow shock (when Titan’s location is outside Saturn’s magnetosphere) and the magnetic barrier due to the large gyroradius of magnetospheric ions. Hybrid simulations provided good results for the TA encounter. However, an understanding and interpretation of the CAPS data for the T9 encounter requires more complicated models of Titan’s atmosphere and ionosphere.

Our study of the neutral atmosphere will be taken from Hartle et al. (2006) and Sittler et al. (2005). Photoionization, electron impact and charge exchange rates were taken from Sittler et al. (2005). We apply a time-dependent Boltzmann’s “particle in cell” approach (Lipato et al., 1998), together with a hybrid plasma (ion kinetic) model (Lipato et al., 2002) in three spatial dimensions (see, e.g. Lipatov and Combi, 2006) using a prescribed but adjustable neutral atmosphere and ionosphere model for Titan. A Boltzmann simulation is applied to model charge exchange between (incoming and pickup) ions and the immobile atmospheric neutrals. In this paper we discuss the first results of a hybrid kinetic simulation of Titan’s environment, namely, global plasma structures, e.g., the formation of a magnetic barrier, Alfvén wing, pickup ion tail etc. The results of these kinetic simulations are compared with Cassini T9 flyby observational data (CAPS). Comparison of results of our hybrid simulation with other Cassini flybys will be presented in a future publication.

The paper is organized as follows: in Section 2 we present the computational model and a formulation of the problem. In Section 3 we present the results of modeling the plasma environment near Titan and comparison with observational data. Finally, in Section 4 we summarize our results and discuss the future development of our computational model.

2. Formulation of the problem and mathematical model

To study the interaction of Saturn’s magnetosphere with the ionized and neutral components of Titan’s environment we use a quasineutral hybrid model, namely, a kinetic description for the background and pickup ions, and a fluid approximation for electrons. The hybrid model accurately describes wave–particle interactions on the following ion spatial (λ) and time (ω^{-1}) scales: $\lambda \sim \rho_{ci} = U_0/\Omega_i$ or $\lambda \sim c/\omega_{pi}$ and $\lambda \gg \rho_{ce}$; $\omega \leq \Omega_i$, where ρ_{ci} and ρ_{ce} denote the gyroradii for ions and electrons (respectively); U_0 is the bulk velocity of the background plasma; c/ω_{pi} denotes the ion inertial length, and Ω_i is the ion gyrofrequency. The length λ may represent either the wave-length of the excited low-frequency waves or the spatial scale of the plasma structures and boundaries in the Titan environment. The model includes photoionization, electron impact ionization and charge exchange. We explicitly include ionization, mass-loading and charge exchange as the dominant mechanisms for the interaction away from the lower boundary at Titan. We also include finite conductivity, given by the diffusion scale length, at the inner boundary. The atmosphere is considered to be an immobile component in this paper.

The general scheme of the global interaction of Saturn’s magnetosphere with Titan and the Cassini T9 trajectory is given in Fig. 1. The Cassini T9 flyby occurred nearly in the equatorial plane of Titan and perpendicular to the direction of the plasma wake defined by the corotating plasma flow past Titan. The spacecraft trajectory passed approximately 10,768 km ($4.2R_T$) downstream from Titan (in the sense of the plasma torus flow). In our coordinate system the X -axis is parallel to U_0 (corotational plasma velocity), Y is directed toward Saturn, and Z is directed to the north.

In the hybrid simulations described here, the dynamics of upstream ions and implanted ions is a kinetic approach, while the dynamics of the electrons is described by a hydrodynamical approximation.

The single particle ion distribution function $f_s(t, \mathbf{x}, \mathbf{v})$ has to fulfill the Vlasov/Boltzmann equation

$$\frac{\partial}{\partial t} f_s + \mathbf{v} \cdot \frac{\partial}{\partial \mathbf{x}} f_s + \frac{\mathbf{F}}{M_s} \cdot \frac{\partial}{\partial \mathbf{v}} f_s = F_{coll} + P - L_{exch}, \quad (1)$$

where \mathbf{F} symbolizes forces due to electric and magnetic fields acting on the ions, F_{coll} is the collision term, P denotes the production rate of the ions by an ionization and charge exchange, and L_{exch} the loss rate of ions due to charge exchange at (\mathbf{x}, \mathbf{v}) . M_s is a mass of an ion of species s . In this paper we use the particle-mesh model for ion dynamics instead of the Vlasov/Boltzmann equation, Eq. (1).

Single ion particle motion is described by the equations (see, e.g. Eqs. (1) and (14) from Mankofsky et al., 1987):

$$\frac{d\mathbf{r}_{s,l}}{dt} = \mathbf{v}_{s,l} \quad (2)$$

and

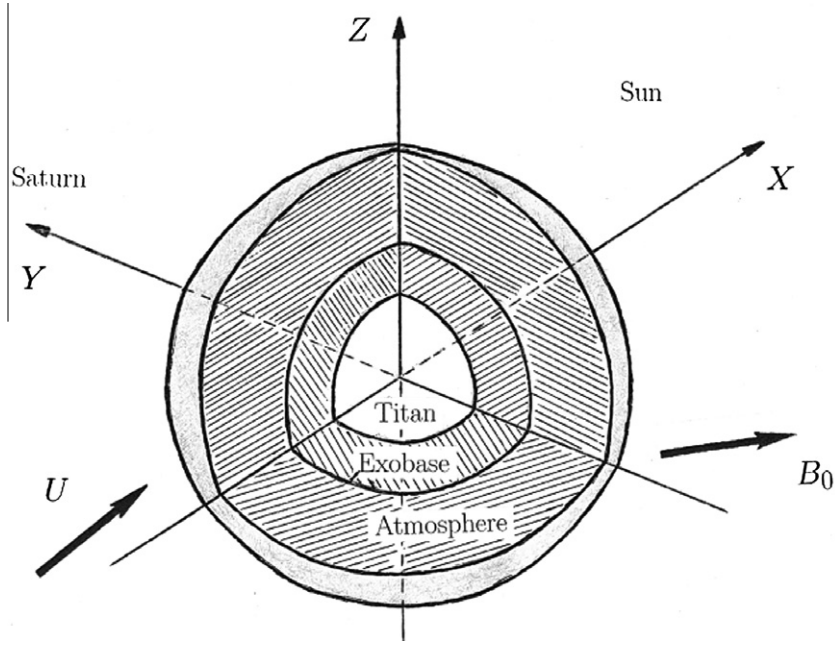


Fig. 1. Titan's plasma environment and the system of coordinates.

$$\frac{d\mathbf{v}_{s,l}}{dt} = \frac{e}{M_s} \left(\mathbf{E} + \frac{\mathbf{v}_{s,l} \times \mathbf{B}}{c} \right) - \frac{m_e v_{ie}}{M_s} (\mathbf{v}_{s,l} - \mathbf{U}_i) - \frac{m_e v_{ie}}{M_s e n_i} \mathbf{J} - v_{so} \mathbf{v}_{s,l}. \quad (3)$$

Here we assume that the charge state is $Z_i = 1$. \mathbf{U}_i and \mathbf{J} denote the charge-averaged velocity of all (incoming and pickup) ions and the total current (see Eq. (8)). Here m_e , e , and n_i are the electron mass, electron charge, and the total ion density (respectively). The subscript s denotes the ion population ($s = 1$ for incoming ions and $s = 2, 3, 4, 5$ for H^+ , H_2^+ , N_2^+ , CH_4^+ pickup ions; $s = 6$ for ionospheric ions) and the index l is the particle index. v_{ie} and v_{io} are collision frequencies between ions and electrons, and ions and neutrals that may include Coulomb collisions and collisions due to particle-wave interactions. Note that the collision rates used in Eq. (3) must depend on individual velocities of ions and electrons. However, we use the effective resistivity η , $\eta = \sigma^{-1} = m_e / (n e^2 \tau_e)$, where the characteristic electron collision time $\tau_e = v_{ie}^{-1}$ and n denotes the total ion density. The electrical conductivities may be estimated as

$$\sigma_{\perp} = \sigma_1 T_e^{3/2}, \quad \sigma_{\parallel} = 1.92 \sigma_{\perp}, \quad \sigma_1 = 0.9 \times 10^{13} / ((A/10) Z_i) \text{ s}^{-1} \text{ eV}^{-3/2}, \quad (4)$$

where T_e denotes the electron temperature in eV and A is the Coulomb logarithm (see, e.g., pp. 215–216 of Braginskii, 1965). For the typical background (upstream) plasma parameters are $T_e = 200$ eV (electron temperature) and $n_0 = 0.1 \text{ cm}^{-3}$ (ion density); the electrical conductivities are $\sigma_{\perp} \approx 4.7 \times 10^{13} \text{ s}^{-1}$ and $\sigma_{\parallel} \approx 9.2 \times 10^{13} \text{ s}^{-1}$. Charged particle-neutral collision frequencies are calculated depending on the species in question. For a plasma, the thermal velocity $v'_\alpha (\alpha = i, e)$ is assumed to be greater than the drift velocity, so we take

$$v_{\alpha,0} = n_0 \sigma^{\alpha,\alpha} v'_\alpha, \quad (5)$$

where the cross section $\sigma^{\alpha,\alpha}$ is typically about $5 \times 10^{-15} \text{ cm}^2$ and n_0 is the neutral atmosphere density (see, e.g., Eq. (17) from Mankofsky et al., 1987).

In our simulation we use a low (much smaller than the real value) effective conductivity to suppress “shot” noise and for modeling Titan’s body; hence, we may drop the first collision term in the right hand side of Eq. (3) for simplicity. We also drop the third collisional term in Eq. (3) for simplicity. We also take into account the interaction of ions with neutral particles by charge exchange (see Eqs. (12)–(15) from Lipatov and Combi (2006)), and we also assume that the bulk velocity and thermal temperatures of neutral particles equal zero.

In the nonradiative limit, Ampère’s law is given by

$$\frac{4\pi}{c} \mathbf{J} = \nabla \times \mathbf{B}; \quad (6)$$

and the induction equation (Faraday’s law) by

$$\frac{1}{c} \frac{\partial \mathbf{B}}{\partial t} + \nabla \times \mathbf{E} = 0. \quad (7)$$

The total current is given by

$$\mathbf{J} = \mathbf{J}_e + \mathbf{J}_i; \quad \mathbf{J}_i = \sum_{s=1}^{N_{\text{species}}} e n_s \mathbf{U}_s = e n_i \mathbf{U}_i, \quad (8)$$

where \mathbf{U}_s is the bulk velocity and n_i is the density of ions of type s ; n_i is the total ion density, and \mathbf{U}_i is the average ion bulk velocity.

We further assume quasi-neutrality

$$n_e = \sum_{s=1}^{N_{\text{species}}} n_s. \quad (9)$$

For massless electrons the equation of motion of the electron fluid takes the form of standard generalized Ohm's law (e.g. Braginskii, 1965):

$$\mathbf{E} = \frac{\mathbf{J}_e \times \mathbf{B}}{en_e c} - \frac{\nabla p_e}{en_e} - \frac{m_e}{e} \sum_s v_{e,s} \left(\mathbf{U}_i - \mathbf{U}_s - \frac{\mathbf{J}}{en_e} \right) - \frac{m_e v_{a,eo}}{e} \mathbf{U}_e, \quad (10)$$

where $p_e = nm_e \langle v_e'^2 \rangle / 3 = n_e T_e$ is the scalar electron pressure, and v_e' is the thermal velocity of electrons; the electron current J_e is estimated from Eq. (8). Evaluation of the effective conductivities that correspond to the frequency $v_{e,o}$ gives the following expression:

$$\sigma_{e,o} = \frac{\omega_{pe}^2}{4\pi v_{e,o}} = \frac{\omega_{pe}^2}{4\pi \sigma_{e,o} n_o' v_e'} = \frac{1.64 \times 10^{14} n_e'}{n_o'} s^{-1}, \quad (11)$$

where dimensional values are $n_e' = n_e/n_0$ (electron density) and $n_o' = n_o/n_{\text{atmos}}$ (neutral density, see Eq. (13)). Here ω_{pe} is the electron plasma frequency and n_0 is the ion background density. In our simulation we assume that $|\mathbf{U}_i - \mathbf{U}_s| \ll J/(ne)$ and we drop the third and fifth terms from the right side of Eq. (10).

Since we suppose that electron heating due to collisions with ions is very small, the electron fluid is considered adiabatic. For simplicity we assume that the total electron pressure may be represented as a sum of partial pressures of all electron populations:

$$p_e \propto \frac{(\beta_e n_{i,up}^{5/3} + \sum_s \beta_{e,PI,s} n_{i,PI,s}^{5/3} + \beta_{e,iono} n_{i,iono}^{5/3})}{\beta_e}, \quad (12)$$

where β_e , $\beta_{e,PI,s}$, and $\beta_{e,iono}$ denote electron upwind, pickup and ionosphere betas. We also assume here that $n_{e,up} = n_{i,up}$, $n_{e,PI,s} = n_{i,PI,s}$, and $n_{e,iono} = n_{i,iono}$. Here, $n_{i,iono}$ denotes the immobile ionosphere ions. Otherwise, we have to calculate the electron pressure from heat balance for electrons (see, e.g., Braginskii, 1965) taking into account the heat fluxes for pickup electrons and ionospheric electrons on the right side of this equation. The ion kinetic approach allows us to take into account the effects of anisotropy of ion pressure, the correct mass loading processes, the penetration of ions across the ionosphere, and the asymmetry of plasma flow around Titan. Remember that the fluid models, which account only for the scalar (i.e., isotropic) ion pressure, may result in an extra-expansion of the pickup ions along the Alfvén wing. Our computational model may also include charge exchange between magnetospheric ions and atmospheric atoms, and between pickup ions and atmospheric atoms (see, e.g., Lipatov and Combi, 2006).

The neutral atmosphere of Titan serves as a source of new ions, mainly by electron impact ionization from the magnetosphere plasma and also by photoionization. The neutral atmosphere also serves as collisional targets for charge exchange with the magnetospheric H^+ and H_2^+ ions. The impacting ions consist both of upstream torus ions as

well as newly implanted ions which are picked up by the motional electric field.

We have adopted a four-species description for the neutral exosphere of the Chamberlain's form

$$n_{\text{neutral},k} \approx n_{\text{atmos},k} \exp(-(1/r - 1/r_{\text{exobase}})h_{\text{atmos},k}). \quad (13)$$

This represents a numerical approximation of the model of exosphere model for Titan (see e.g. Amsif et al., 1997 and Fig. 18 from Sittler et al., 2010). In Eq. (13), $n_{\text{atmos},k}$ is the maximum value of the neutral density extrapolated to the exobase, and $r_{\text{exobase}} \approx 4000$ km (Yelle et al., 2006). Index k denotes H, H_2 , CH_4 , and N_2 . Here the spatial scales are $h_{\text{atmos,H}} = 2.2 \times 10^4$ km, $h_{\text{atmos,H}_2} = 2.75 \times 10^4$ km, $h_{\text{atmos,CH}_4} = 8.3 \times 10^4$ km and $h_{\text{atmos,N}_2} = 1.77 \times 10^5$ km. The thermal velocity of all newly formed pickup ions is about 0.25 km/s.

We use a model of the ionosphere that contains a shell-like immobile ionosphere at the Sun side at $R_{\text{iono}} = 1300$ km + R_T :

$$n_{\text{iono}} \approx n_{\text{iono},R_{\text{iono}}} \exp(-(r - R_{\text{iono}})^2/\delta_{\text{iono}}^2) \quad (14)$$

and simulate the ionospheric ion flux using active ion macro-particles with $M_i = 28$ amu:

$$\text{flux}_{\text{iono}} \approx \text{flux}_{\text{iono},R_{\text{iono}}} \exp(-(r - R_{\text{iono}})^2/\delta_{\text{iono}}^2), \quad (15)$$

Here $\delta_{\text{iono}} = 200$ km is a characteristic spatial scale for the thickness of the ionosphere, and the total flux though ionosphere is about 5×10^{25} ion/s. Note that an immobile ionosphere with $n_{\text{iono},R_{\text{iono}}} = 6.25$ ion/cm³ is used in the simulation to avoid a low value of density due to fluctuations in particle-in-cell method.

The production of new ions from the exosphere near Titan corresponds to

$$G_{\text{exo},k} \propto v_{i,k} n_{\text{atmos},k} \exp[(1/r - 1/r_{\text{exobase}})h_{\text{atmos},k}]. \quad (16)$$

Here $n_{\text{atmos},k}$ denotes the value of the neutral component density at $r = r_{\text{exobase}}$ and $v_{i,k}$ is the effective ionization rate per atom or molecule of species k , which includes the photoionization v_{ph} , and the electron impact ionization by the background $v_{e,im}$ and the secondary $v_{e^*,im}$ electrons.

2.1. Initial conditions

Initially the computational domain contains only subAlfvén and subsonic background plasma flow with a homogeneous spatial distribution and a Maxwellian velocity distribution; the pickup ions have a weak density and spherical spatial distribution. The magnetic field and electric fields are $\mathbf{B} = \mathbf{B}_0$ and $\mathbf{E} = -\mathbf{U}_0 \times \mathbf{B}_0/c$. Inside Titan the electromagnetic fields are $\mathbf{E} = 0$ and $\mathbf{B} = \mathbf{B}_0$, and the bulk velocities of ions and electrons also equal to zero.

At $t > 0$ we begin to inject the pickup ions with a distribution according to Eq. (16). Far upstream ($x = -13L$, where $L = R_T$), the ion flux is assumed to have a Maxwellian distribution,

$$f = n_{\infty}(\pi v_{th}^2)^{-3/2} \exp \left[-\frac{(\mathbf{v} - \mathbf{U})^2}{2v_{th}^2} \right], \quad (17)$$

where v_{th} and \mathbf{U} are the thermal and the bulk velocities of the background plasma flow, respectively.

2.2. Boundary conditions

At the side boundaries we use a damping boundary condition for the electromagnetic field. At the back boundary we use a “Sommerfeld” radiation condition for the magnetic field, and a free escape condition for particles, with re-entry of a portion of the particles from the outflow plasma. The magnetic field and electric fields are $\mathbf{B} = B_0$ and $\mathbf{E} = -\mathbf{U}_0 \times \mathbf{B}_0/c$.

Inside Titan, the electromagnetic fields are $\mathbf{E} = 0$ and $\mathbf{B} = \mathbf{B}_0$, and the bulk velocities of ions and electrons also equal to zero.

We also take into account the effect of the finite conductivity of Titan’s body so that

$$\begin{aligned} \sigma_{eff} &= \sigma_{up}, & \text{for } r > R_T + H_{atmos}, \\ \sigma_{eff} &= \sigma_{iono}, & \text{for } R_T < r \leq R_T + H_{atmos}, \\ \sigma_{eff} &= \sigma_T, & \text{for } r \leq R_T. \end{aligned}$$

Our code solves Eqs. (1)–(17).

Far downstream, we adopted a free escape condition for particles and Sommerfeld’s radiation condition for the magnetic field. On the side boundaries ($y = \pm DY/2$ and $z = \pm DZ/2$), periodic boundary conditions were imposed for incoming flow particles and the electromagnetic field. The pickup ions exit the computational domain when they intersect the surfaces $y = \pm(DY/2 - 5 \times \Delta y)$, or $z = \pm(DZ/2 - 5 \times \Delta z)$, or $x = 14L - 5 \times \Delta x$. Thus there is no influx of pickup ions at the side boundaries. At Titan’s surface, $r = R_T$, the particles are absorbed. There is no boundary condition for the electromagnetic field, and we also use our equations for the electromagnetic field, Eqs. (4), (5) and (10) inside Titan but with internal conductivity and the bulk velocity that is calculated from the particles. In this way the jump in the electric field is due to the variation of the value of the conductivity and bulk velocity across Titan’s surface. Note that the position of Titan is $x = 0$, $y = 0$, $z = 0$.

The three-dimensional computational domain has dimensions $DY = 30L$, $DZ = 30L$, and $DX = 27L$, where $L = R_T = 2575$ km. We used meshes of $301 \times 301 \times 276$ grid points, and 4.5×10^8 and 8×10^7 particles for protons and pickup ions, respectively, for a homogeneous mesh computation. The time step Δt satisfies the condition $v_{max}\Delta t \leq \min(\Delta x, \Delta y, \Delta z)/8$.

The relationship between dimensional (U, E, B, p_e, n, T) and dimensionless (U', E', B', p'_e, n', T') parameters may be expressed via the dimensional upstream values as follows:

$$\begin{aligned} \mathbf{U} &= \mathbf{U}'U_0, & \mathbf{E} &= \mathbf{E}'B_0U_0/c, & \mathbf{B} &= \mathbf{B}'B_0, & p_e &= p'_e p_{e0}, \\ n &= n'n_0, & T &= T'M_iU_0^2, \end{aligned} \quad (18)$$

whereas the dimensional time and distance may be expressed via the bulk velocity U_0 and characteristic scale $L = R_T$:

$$t = t'L/U_0, \quad \mathbf{x} = \mathbf{x}'L. \quad (19)$$

The global physics in Titan’s environment is controlled by a set of dimensionless independent parameters such as M_A , β_i , β_e , M_{PI}/M_p , ion production and charge exchange rates, diffusion lengths, and the ion gyroradius $\epsilon = \rho_{ci}/R_T$. Here $\rho_{ci} = U_0/(eB/M_i c)$ and the ion plasma frequency $\omega_{pi} = \sqrt{4\pi n_0 e^2/M_i}$. For real values of the magnetic field the value of the H_2^+ background ion, H_2^+ and CH_4^+ pickup ion gyroradii are about 200–400 km, 200–400 km and 1500–3000 km (respectively) which are calculated from the local bulk velocity. The grid spacing has the value $\Delta_x = 257.5$ km.

In order to study ion kinetic effects (e.g. excitation of low-frequency oscillations ($\omega \ll \Omega_b$) by the mass loading), we must satisfy the condition $\Delta \leq (10 - 20)c/\omega_{pb}$, where Ω_b and ω_{pb} denote the gyrofrequency and the plasma frequency for background ions (Winske et al., 1985). The above estimation of the plasma parameters shows that we have good resolution for the low-frequency waves. To excite high-frequency waves ($\Omega_b \ll \omega \ll \Omega_e$) we must satisfy the condition $\Delta \leq 0.25c/\omega_{pb}$, (Winske et al., 1985) for background ions. The above estimation shows that we have insufficient resolution for the high-frequency waves.

3. Results of the simulation

To study the interaction of Saturn’s magnetospheric ions with the ionosphere of Titan the following sets of the magnetospheric plasma and ionosphere parameters were adopted in accordance with flyby observational data: upstream velocity, densities and magnetic field: $U_0 = 201$ km/s; $V_0 = -91.4$ km/s; $W_0 = 0$ km/s; $n_{H_2^+} = 0.05$ cm $^{-3}$; $B_0 = 5.59$ nT; $\mathbf{B}/B_0 = (0.46, 0.82, -0.34)$; $T_{H_2^+} = 201$ eV; $M_A = 0.75$; $M_S = 0.67$; $\beta_{H_2^+} = 0.35$; $\beta_{e,0} = 1$; ($T_e = 200$ eV); and $\beta_{e,2} = 0.025$ – 0.25 ; ($T_{pickup,e} = 5$ – 50 eV); $\beta_{e,iono} = 0.006$.

In this section we discuss the results of a simulation at time $t = 11 T_{transit}$, where $T_{transit}$ denotes a transition time for particle from the left (upstream) boundary to the right (downstream) boundary.

3.1. Global structure of Titan’s environment (T9 encounter)

The simulation shows the formation of the Alfvén wing oblique to the y -axis in the background ion density profile, Fig. 2 (left, top). The top part of the wing has a plane front whereas the bottom part has a more diffuse transition. Note that these Alfvén wings have the same location as the Alfvén wing for the maximum density of H_2^+ and CH_4^+ pickup ions, (compare with Fig. 2 (left, top) and Fig. 3 (left, top and bottom)).

The simulation also demonstrates an asymmetrical front in the density of the background H_2^+ ions in x – y plane. In

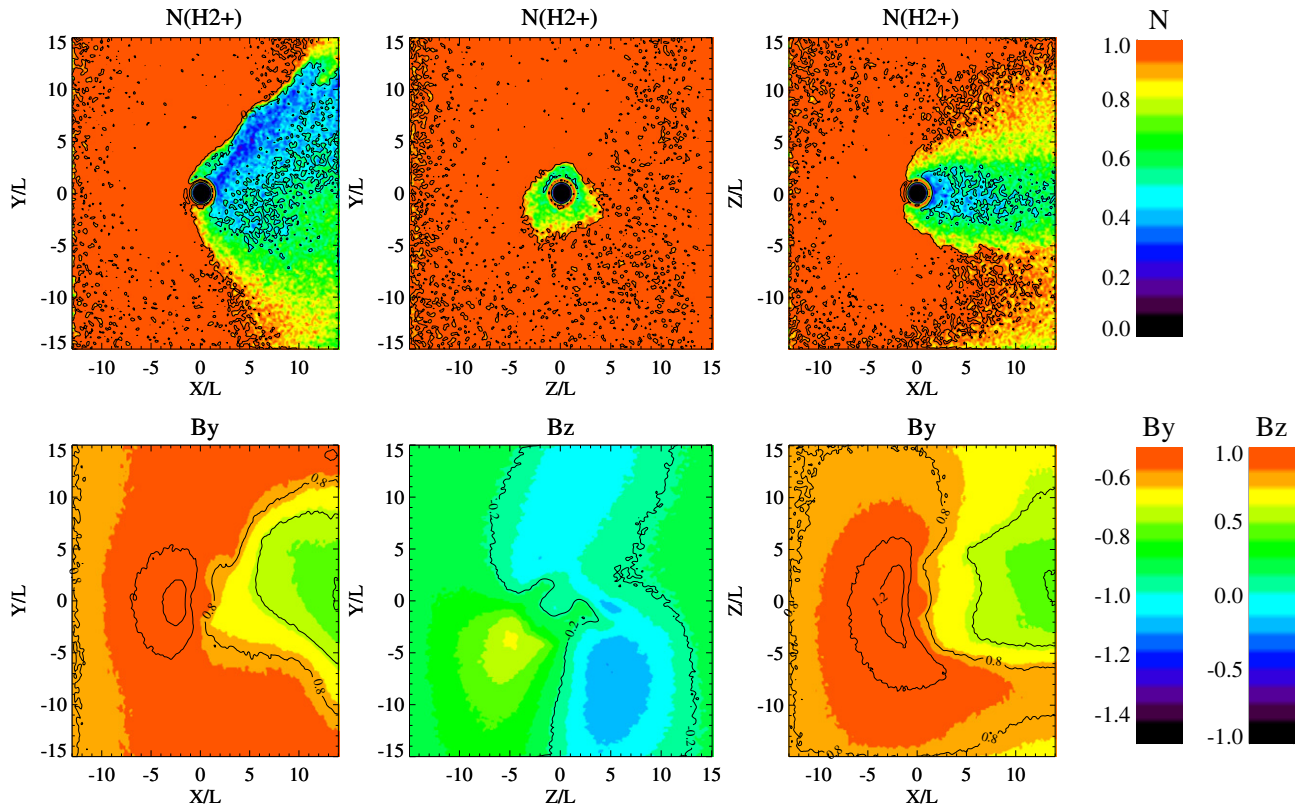


Fig. 2. 2-D cuts of the background H_2^+ ion (top) density profile and the magnetic field (bottom).

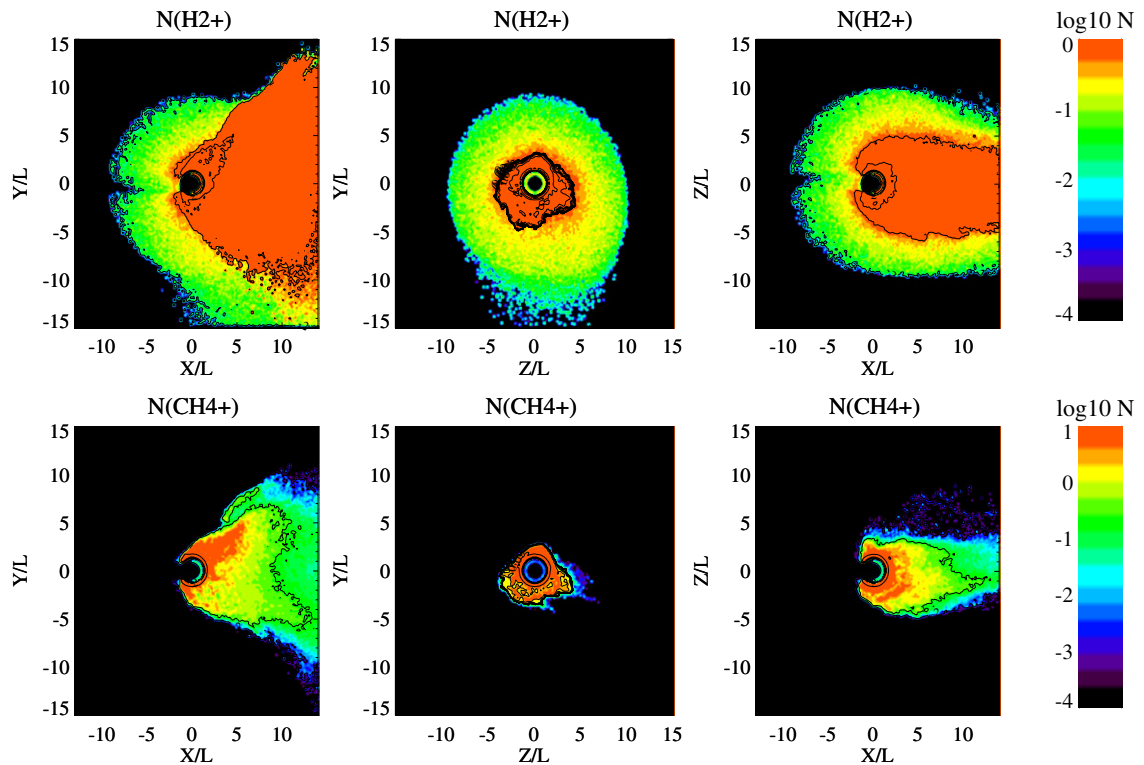


Fig. 3. 2-D cuts of the pickup ion density profile (top H_2^+), (bottom CH_4^+).

the region with $y > 0$ the front transition has a diffuse structure, whereas in the region with $y < 0$ the front transition has a jump-like structure. In our sub-Alfvénic flow the front may be associated with an Alfvén wing. One may see density depletion inside the Alfvén wing. The asymmetrical distribution of the incoming ions in the y – z plane may be explained by the existence of the B_z component of the upstream magnetic field. The inclination of the magnetic field results in an asymmetrical boundary condition for ion dynamics (penetration and reflection) in Titan’s ionosphere and an asymmetrical Alfvén wing. The density profile is slightly disturbed near the side boundaries. However, as already discussed, this perturbation does not affect the region close to Titan.

Fig. 2 (top, right) shows the asymmetrical coma-like distribution of pickup ions H^+ . A cone-like higher density distribution of the H_2^+ pickup ions is merged in the coma distribution. The H_2^+ pickup ions are created mostly by photoionization and electron impact ionization. The motion along the magnetic field is due to the thermal velocity and the gradient of the electron pressure. At the front of the Alfvén wing one may see a strong gradient in the density of pickup ions.

Fig. 3 (right, bottom) shows a plasma wake for a CH_4^+ pickup ion distribution. CH_4^+ pickup ions create a double-tail structure due to the parallel electric field. Near the exobase, the parallel electric field is mainly determined by the electron pressure and it is oriented out of exosphere. Note that the mechanism results in splitting of the plasma wake near a small comet (see e.g. Lipatov, 2002).

The results of the measurements by the particles and field instruments on the Cassini spacecraft during the T9 encounter provided new and important information with which realistic simulations for the plasma interaction can

be tested. Along that trajectory physical signatures of the wake were seen as one sharp strong peak (event 1) and a broad weak peak (event 2) in the pickup ion density.

Fig. 4 shows the total density of the pickup ions along the Cassini trajectory from the CAPS measurements (●) (Sittler et al., 2009, 2010). The densities of the pickup ions and upstream ions produced in the 3D hybrid simulations are also shown: the total pickup ions density – $N_{pi,tot}$ (solid line), the light pickup ion density – H^+ (Δ) and H_2^+ (*), the heavy pickup ion densities – N_2^+ (\diamond) and CH_4^+ (\times), the active ionospheric ion density – $M = 28$ amu (\circ), and the background ion density (\square). Here, $S_y(R_T)$ denotes the projection of the spacecraft trajectory onto the y -axis.

The simulation produces a total pickup ion density profile that has a maximum value very close to the peak in the density observed in event 1, Fig. 4 (solid line). The total ion density profile agrees well with that derived from the upper hybrid resonance frequency combined with the Langmuir probe observations from Modolo et al. (2007b). The total ion density produced in the hybrid simulation of Modolo et al. (2007a) also show a good agreement with the RPWS experiment. However, the inbound and outbound values of total density are higher by factor of 5–10 than observed values. The main peak of the total ion density in the simulation of Modolo et al. (2007a) is smaller by a factor of 2.5 than the observed value. These differences in the total ion density may be explained by an inclusion of heavy O^+ in the background plasma in simulation.

The main input in the peak value is due to H_2^+ , CH_4^+ and N_2^+ pickup ions. In event 2 the value of the model’s density exceeds the observation data and therefore is only in qualitative agreement with observation. We do not observe a depletion in the total ion density profile at $S_y(R_T) = 0$ in Fig. 4. However, some depletion at $S_y(R_T) = 0$ was observed during the simulation due to the plasma wake not being stationary. Here we have discussed only one model for the Titan atmosphere and ionosphere; the other models will be considered in Lipatov et al. (submitted for publication). We should also note that the hybrid simulation for T9 with heavy ions in upstream (see e. g. Simon et al. (2007)) produces another picture of the plasma–Titan interaction because of deeper penetration of these ions into the ionosphere. The MHD and Hall-MHD simulation with light and heavy ions upstream produces only one peak in the plasma density profile between event 1 and event 2, (Ma et al., 2007). However, the CAPS measurements did not confirm the existence of the heavy ions upstream.

3.2. Velocity distribution of the background and pickup ions

The simulation shows a quasi-adiabatic evolution of the quasi-Maxwellian velocity distribution of the H_2^+ background ions due to mass loading (Fig. 5). At distance $y = 4R_T$ the value of the transverse temperature is comparable or larger than the value of the parallel temperature, $T_{\perp,H_2^+}/T_{\parallel,H_2^+} \approx 1.4$ (upstream flow) and $T_{\perp,H_2^+}/T_{\parallel,H_2^+} \approx 0.9$ (downstream flow, event 1) (Table 1). The CAPS

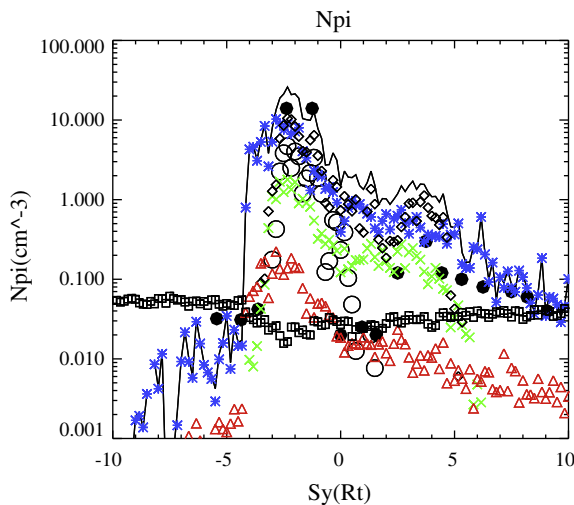


Fig. 4. Pickup ion densities N_{pi} along the Cassini trajectory. CAPS (Sittler et al., 2009) total pickup ion density – (●). Simulation: total pickup ion density – $N_{pi,tot}$ (solid line); partial densities for pickup ions – N_2^+ (\diamond – black), CH_4^+ (\times – green), H_2^+ (* – blue), H^+ (Δ – red); ionospheric $M = 28$ ions (\circ), background H_2^+ ions (\square – black).

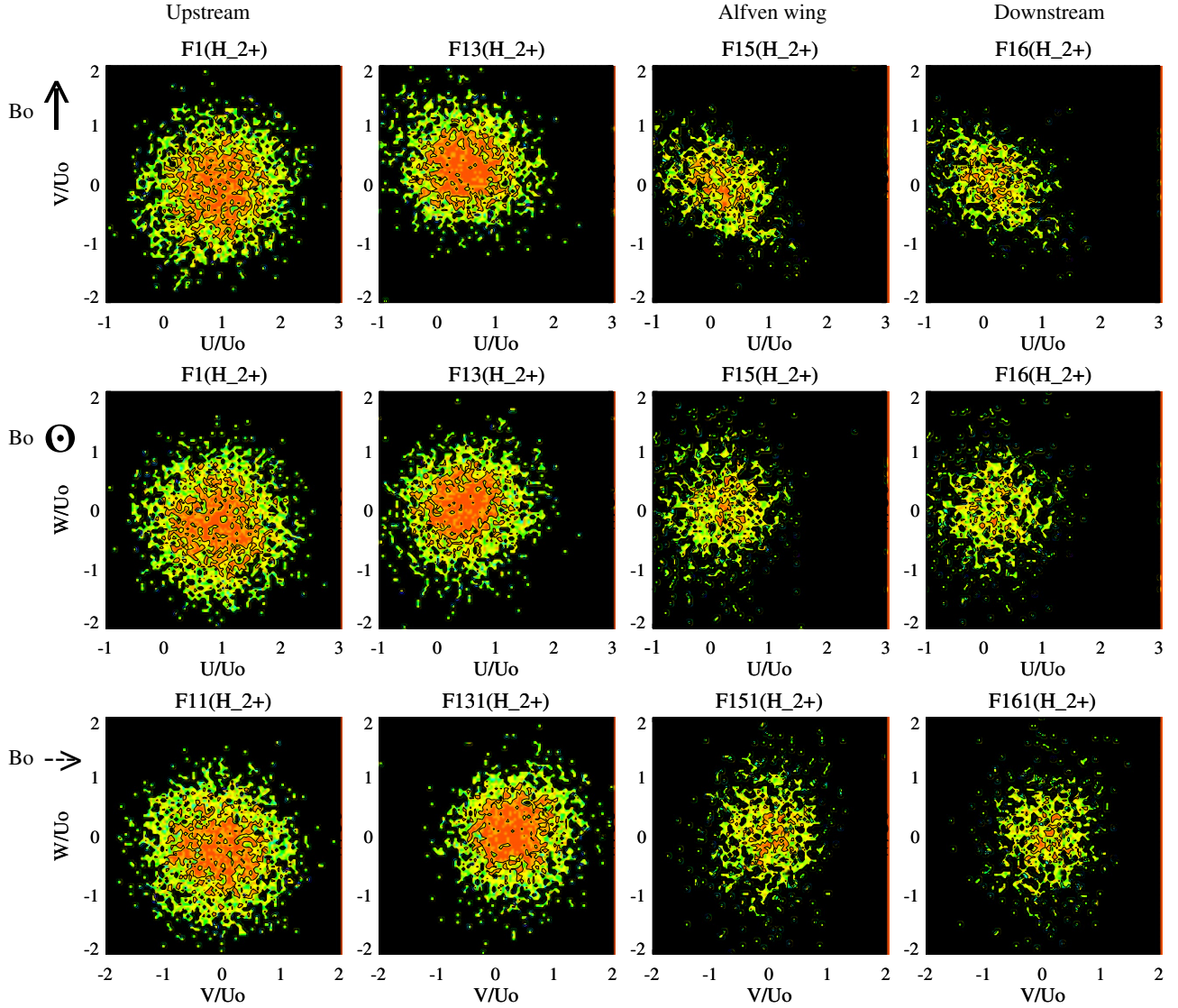


Fig. 5. 2D projection of the velocity distributions ($\log_{10}F$) of the H_2^+ background ions. $Y = 4R_T$. Columns: $X/L = -10.0; 2.0; 3.0; 5.0$. See pickup ion density profile in Fig. 2 (top).

Table 1
Simulation and CAPS observation.

Ions	Event 1		Event 2	
	T (eV)	T_{\perp}/T_{\parallel}	T (eV)	T_{\perp}/T_{\parallel}
H_2^+ (background)	300	0.9	300	0.95
CAPS (H^+)	266	2	57	1.4
H_2^+ (PI)	32	1.13	75	1.8
CAPS (H^+, H_2^+)	145	0.99	14	2
CH_4^+ (PI)	50	1.33–1.75	32	0.83–1.4
CAPS (Mass 16)	4	2	<50	

observations give the temperature anisotropy $T_{\perp,H_2^+}/T_{\parallel,H_2^+} \approx 2.0$ downstream flow (event 1) that is much higher than one can see in simulation. The thermal energies of the background ions are about 300 eV (simulation) and 266 eV (event 1 CAPS observations). At a smaller distance $y = 2R_T$, a stronger compression of the background H_2^+ ions

is observed. For event 2 ($y = +4R_T$) the simulation gives $T_{\perp,H_2^+}/T_{\parallel,H_2^+} \approx 1.2$ (upstream flow) and $T_{\perp,H_2^+}/T_{\parallel,H_2^+} \approx 0.95$ (downstream flow) whereas the CAPS observation gives a higher value of the temperature anisotropy, $T_{\perp,H_2^+}/T_{\parallel,H_2^+} \approx 1.4$. The H_2^+ pickup ion temperatures are 300 eV (simulation) and 57 eV (event 2 observations).

The pickup ion dynamics are very complicated due to the inhomogeneous distribution of the source of these ions. Besides, the mass loading of Saturn's magnetospheric flow by heavy ions results in a strong deceleration of the bulk velocity and the motional electric field. The electromagnetic turbulence may also result in phase mixing and hence the formation of a velocity distribution with a quasi-Maxwellian core and a shell-like halo downstream flow.

In the outer region of the exosphere, the velocity distributions of the H_2^+ pickup ions are ring-like distributions for $z = 0$ and $y = 4R_T$ (Fig. 6). The parallel and perpendicular

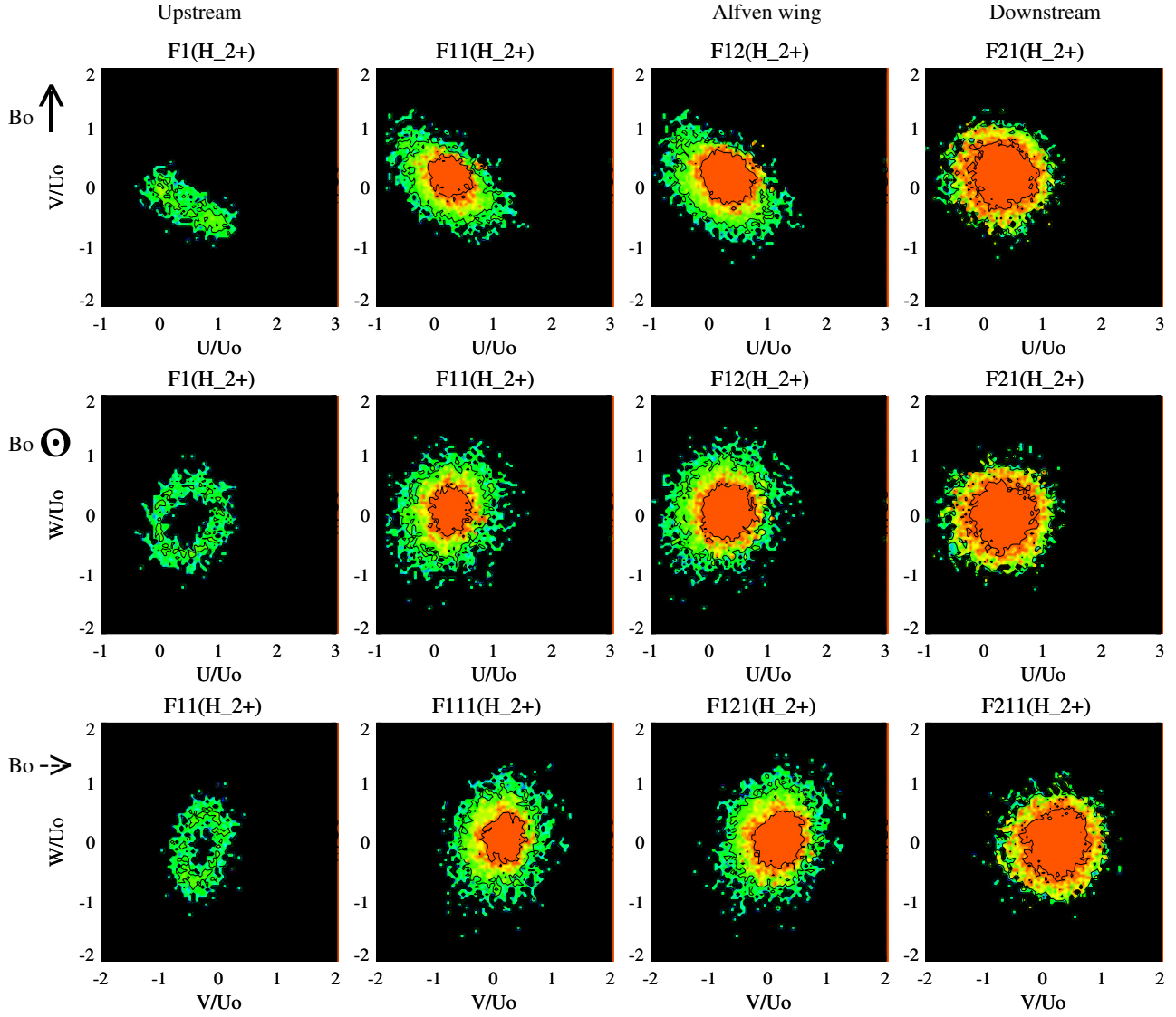


Fig. 6. 2D projection of the velocity distributions ($\log_{10} F$) of the H_2^+ pickup ions. $Y = 4R_T$. Columns: $X/L = -4.0; 1.0; 1.5; 6.0$. See pickup ion density profile in Fig. 3 (top).

velocities of H_2^+ pickup ions are $V_\perp = 2/3 U_0$ and $V_\parallel = 0.4 U_0$, and the bulk velocity of the background H_2^+ ions is about $0.8 U_0$. The simulation shows a strong transformation in the velocity distribution of H_2^+ pickup ions from a quasi-ring distribution to a quasi-Maxwellian core and a shell-like halo. One may observe a diffusion of the particles from the thin ring distribution ($X/L = -4.0$) to a thicker ring distribution along the x -axis. The spatial

relaxation scale for that diffusion is about 25,000 km for the H_2^+ pickup ions. The Maxwellian velocity distribution is connected with creation and pickup acceleration of H_2^+ ions at the region with stronger mass loading and, hence, with stronger reduced bulk velocity of the background H_2^+ ions. Fig. 7 shows 1D cuts ($w = 0$) for the velocity distribution $F = F(v)$ of H_2^+ pickup ions in the form $(\sqrt{-\ln F})$. One can see to a ring distribution (two negative peaks) at

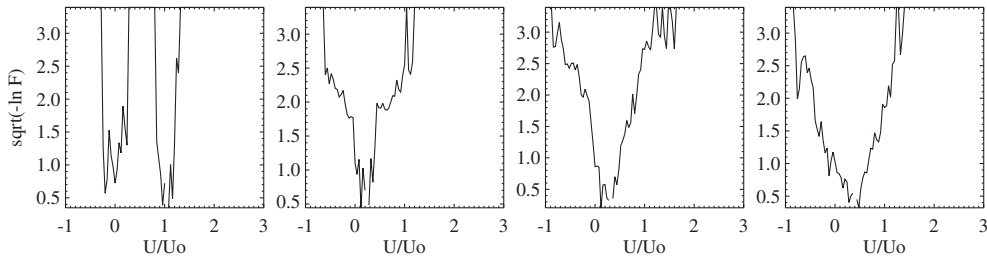


Fig. 7. 1D cuts of the velocity distributions for H_2^+ pickup ions ($\sqrt{-\ln F}$). $Y = 4R_T$. Columns: $X/L = -4.0; 1.0; 1.5; 6.0$.

$X/L = -4.0$, a combination of the Maxwellian distribution (negative peak with linear slopes) and a strong halo (also with two linear slopes) at $X/L = 1.0$, the same combination of the Maxwellian distribution and asymmetrical shell-like halo at $X/L = 1.5$, and finally a quasi-Maxwellian distribution at $X/L = 6.0$. The values of temperature anisotropies are $T_{\perp,H_2^+}/T_{\parallel,H_2^+} \approx (2.3 - 2.5)$ (outer exosphere) and $T_{\perp,H_2^+}/T_{\parallel,H_2^+} \approx 1.13$ (downstream flow). The values of the temperature of the H_2^+ ions are 32 eV (simulation) and 145 eV (event 1 observations). For event 2 the simulation gives the following temperature anisotropy $T_{\perp,H_2^+}/T_{\parallel,H_2^+} \approx 4.0$ (outer exosphere) and $T_{\perp,H_2^+}/T_{\parallel,H_2^+} \approx 1.8$ (downstream flow). The values of the temperature are 185 eV (outer exosphere) and 75 eV (downstream flow).

In the outer region of the exosphere the velocity distributions of the CH_4^+ pickup ions must be ring-like distributions. However, we do not observe these distribution due to inadequate numerical approximation of the generation of

the CH_4^+ pickup ions. On the other hand the CH_4^+ pickup ions begin their motion in the region with small bulk velocity due to mass loading of the background plasma with H_2^+ pickup ions. Fig. 8 shows the variation of the of velocity distribution for CH_4^+ heavy ions along x -axis for $z = 0$ and $y = 4R_T$. The simulation shows a strong transformation in the velocity distribution of the CH_4^+ and N_2^+ pickup ions from a combination of a small shell-like and beam distribution to a quasi-Maxwellian core and a wide shell-like halo downstream flow. The values of CH_4^+ pickup ion temperature anisotropies are about $T_{\perp,CH_4^+}/T_{\parallel,CH_4^+} \approx 2.36 - 1.4$ near the edge of the Alfvén wing, and $T_{\perp,CH_4^+}/T_{\parallel,CH_4^+} \approx 1.33 - 1.75$ in downstream flow (Table 1). The velocity distribution of the N_2^+ heavy pickup ions is very similar to the CH_4^+ velocity distribution. The temperatures of the CH_4^+ pickup ions are 50 eV (simulation) and 4 eV (event 1 observations). For event 2, the simulation gives the following values: $T_{\perp,CH_4^+}/T_{\parallel,CH_4^+} \approx 4.8$ (outer exo-

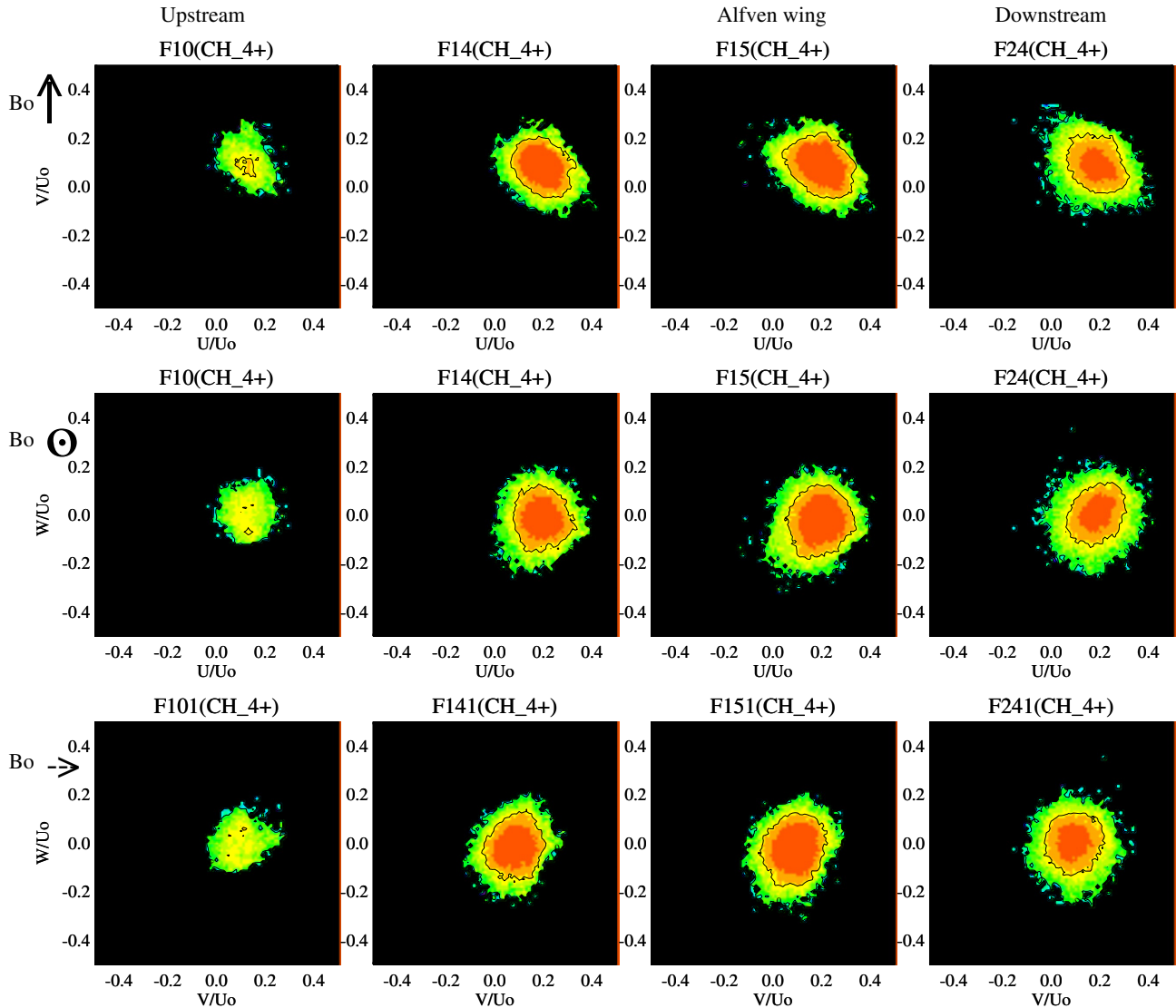


Fig. 8. 2D projection of the velocity distributions ($\log_{10}F$) of the CH_4^+ pickup ions. $Y = 4R_T$. Columns: $X/L = 0.5; 2.5; 3.0; 7.5$. See pickup ion density profile in Fig. 3 (bottom).

sphere), $T_{\perp, \text{CH}_4^+}/T_{\parallel, \text{CH}_4^+} \approx 1.4$ (downstream flow), and $T_{\text{CH}_4^+} = 32$ eV. The velocity distribution of the N_2^+ heavy pickup ions is very similar to the CH_4^+ velocity distribution. Here we have to note that numerical approximation of the distribution of the CH_4 and N_2 components of the atmosphere in the outer region of exosphere is not good enough. To reduce a numerical “shot” noise we have to use a variable mass macro-particles for generation of the heavy pickup ions initial spatial distribution. Unfortunately, the CAPS observation does not produce the heavy ion velocity distribution because of their low flux in the event 2.

This paper derives velocity distributions that are guided by the moments of the velocity distributions of T9 and T18 CAPS data, which are briefly described by Sittler et al. (2010) who will detail these definitions in a subsequent paper (Sittler et al., submitted for publication). Eventually, in future papers this work will be guided directly by CAPS velocity distributions.

The ring-type of the velocity distribution for H_2^+ pickup ions observed in modeling could cause generation of an ion cyclotron waves; however, the background thermalized component of H^+ and H_2^+ will efficiently damp the waves (Cowee et al., 2010). The heavy pickup ions CH_4^+ and N_2^+ from the outer exosphere could also generate the ion cyclotron waves, but their gyroperiods are larger than convection time though the exosphere of Titan (Cowee et al., 2010). In this report, the heavy pickup ions have a quasi-isotropic velocity distribution function and, hence, cannot generate the ion cyclotron waves. Future modeling with variable mass macro-particles will produce a ring velocity distribution for heavy pickup ions and possibly will demonstrate the generation of these waves in the distant plasma wake.

One may also see strong phase mixing in the plasma wake. The plasma wake demonstrates the formation of time-dependent structuring in the pickup ion tails and the splitting of the pickup ion tails. Such finite gyroradius effects were also observed in 2.5 D hybrid and bi-fluid simulations of a weak comet (see, e.g., Lipatov et al., 1997, Sauer et al., 1996, 1997, Lipatov, 2002).

4. Conclusions

- The simulation shows a quasi-adiabatic evolution of the velocity distribution of the background ions $T_{\perp}/T_{\parallel} \approx 1.4 - 0.9$ (event 1) and $1.2 - 0.95$ (event 2) due to mass loading.
- The simulation shows a strong transformation in the velocity distribution of the H_2^+ pickup ions $T_{\perp}/T_{\parallel} \approx 2.25 - 1.3$ (event 1) and $4.4 - 1.8$ (event 2), and for the CH_4^+ pickup ions $T_{\perp}/T_{\parallel} \approx 2.4 - 1.75$ (event 1) and $4.8 - 1.4$ (event 2) near the edge of the Alfvén wing. (From quasi-ring distribution to quasi-Maxwellian core and shell-like halo).
- The relaxation spatial scales are about 25,000 km for the H_2^+ pickup ions.

- The ratios $T_{\text{H}_2^+, \perp}/T_{\text{H}_2^+, \parallel}$ for background ions and $T_{\text{CH}_4^+, \perp}/T_{\text{CH}_4^+, \parallel}$ for heavy pickup ions are smaller in the hybrid simulation than were observed in CAPS measurements (event 1). The ratio $T_{\text{H}_2^+, \perp}/T_{\text{H}_2^+, \parallel}$ for pickup ions is larger in the hybrid simulation than was observed in CAPS measurements (event 1).
- The values of energy $T_{\text{H}_2^+}$ for background ions and $T_{\text{CH}_4^+}$ for pickup ions are larger in the hybrid simulation than were observed in CAPS measurements (event 1). The value of energy $T_{\text{H}_2^+}$ for pickup ions is smaller in the hybrid simulation than were observed in CAPS measurements (event 1).
- The non-Maxwellian velocity distribution may serve as a key factor in the interaction between ions and the neutral component in Titan’s environment.
- Our model produces a satisfactory agreement with observation of the total pickup ion (event 1) and background ion density. For event 2, the simulation produces a higher peak in the density profile. The simulation did not produce a strong gap between the peaks in the density profile for event 1 and event 2.
- The essential part of our simulation is an absence of the heavy ions in the background plasma in accordance with the CAPS measurements. The hybrid simulations for the T9 case with heavy ions upstream (see e. g. Simon et al., 2007, Modolo et al., 2007a) produces another picture of plasma-Titan interaction because of deeper penetration of the heavy background ions into the ionosphere. The MHD and Hall-MHD models, which also include the heavy ions in the background plasma, produce only one wide peak in the density profile between events 1 and 2, Ma et al. (2007).
- Our realistic 3D kinetic simulation must be compared in detail with a 1-D kinetic simulation that was performed with a fine spatial resolution (Cowee et al., 2010).
- Future simulations must use the composite grid structure, e.g. “Cubed sphere”, “Yin-Yang” grids (see, e.g., Koldoba et al., 2002, Kageyama and Sato, 2004; and references therein) to resolve the multiscale effects near the surface of Titan and in outer plasma environment. These approaches will allow us to delete the effects of the reflection of the waves on the side boundaries. These simulations will also allow us to study some kinetic wave-particle interaction effects in the plasma wake, such as the ion cyclotron waves that expect to observe in a distant plasma wake.

Acknowledgments

A.S.L., E.C.S., R.E.H., J.F.C., and D.G.S. were supported by the Grant *Analysis of Titan’s Interaction with Saturn’s Magnetosphere using Cassini Titan Flyby Data and Kinetic-Fluid Model* from the NASA Cassini Data Analysis Program (08-CDAP08-0043). A.S.L. was also supported in part by the Grants/Tasks 900-37-172 and 670-90-315 between the GEST Center UMBC and NASA GSFC.

Computational resources were provided by the NASA Ames Advanced Supercomputing (NAS) Division (Projects SMD-09-1124 and SMD-10-1517). The authors thank the referees for fruitful comments.

References

- Amsif, A., Dandouras, J., Roelof, E.C. Modeling the production and imaging of energetic neutral atoms from Titan's exosphere. *J. Geophys. Res.* 102 (A10), 22169–22181, 1997.
- Braginskii, S.L. Transport processes in a plasma, in: Leontovich, M.A. (Ed.), *Reviews of Plasma Physics*. Consultants Bureau, New York, pp. 205–240, 1965.
- Brecht, S.H., Luhmann, J.G., Larson, D.J. Simulation of the Saturnian magnetospheric interaction with Titan. *J. Geophys. Res.* 105 (A6), 13119–13130, 2000.
- Cowee, M.M., Gary, S.P., Wei, H.Y., Tokar, R.L., Russell, C.T. An explanation for the lack of ion cyclotron wave generation by pickup ions at Titan: 1-D hybrid simulation results, *J. Geophys. Res.* 115, A10224, doi:10.1029/2010JA015769, 2010.
- Cravens, T.E., Lindgren, C.J., Ledvina, S.A. A two-dimensional multifluid MHD model of Titan's plasma environment. *Planet. Space Sci.* 46 (9/10), 1193–1205, 1998.
- Hartle, R.E., Sittler, E.C., Neubauer, F.M., et al. Initial interpretation of Titan plasma interaction as observed by the Cassini plasma spectrometer: comparisons with Voyager 1. *Planet. Space Sci.* 54, 1211–1224, 2006.
- Kabin, K., Gombosi, T., De Zeeuw, D., Powell, K., Israelevich, P. Interaction of the Saturnian magnetosphere with Titan: results of a three-dimensional MHD simulation. *J. Geophys. Res.* 104 (A2), doi:10.1029/1998JA900080.6536, 1999.
- Kabin, K., Israelevich, P., Ershkovich, A., Neubauer, F., Gombosi, T., De Zeeuw, D., Powell, K. Interaction of the Saturnian magnetosphere with Titan: results of a three-dimensional MHD simulation. *J. Geophys. Res.* 104 (A2), doi:10.1029/1998JA900080.6536, 2000.
- Kageyama, A., Sato, T. Yin-Yang grid: an overset grid in spherical geometry. *Geochemistry, Geophysics and Geosystems* 5 (9), Q09005, doi:10.1029/2004GC000734, 2004.
- Kallio, E., Sillanpää, I., Janhunen, P. Titan in subsonic and supersonic flow. *Geophys. Res. Lett.* 31, L15703, doi:10.1029/2004GL020344, 2004.
- Kallio, E., Sillanpää, I., Jarvinen, R., Janhunen, P., Dougherty, M., Bertucci, C., Neubauer, F. Morphology of the magnetic field near Titan: Hybrid model study of the Cassini T9 flyby. *Geophys. Res. Lett.* 34, L24S09, doi:10.1029/2007GL030827, 2007.
- Keller, C.N., Cravens, T.E. One-dimensional multispecies hydrodynamic models of the wakeside ionosphere of Titan. *J. Geophys. Res.* 99 (A4), 6527–6536, 1994.
- Koldoba, A.V., Romanova, M.M., Ustyugova, G.V., Lovelace, R.V.E. Three dimensional MHD simulation of accretion to an inclined rotator: the “cubed sphere” method. *Astrophys. J.* 576, L53–L56, 2002.
- Ledvina, S.A., Cravens, T.E. A three-dimensional MHD model of plasma flow around Titan. *Planet. Space Sci.* 46 (9/10), 1175–1191, 1998.
- Lipatov, A.S. The Hybrid Multiscale Simulation Technology: An Introduction with Application to Astrophysical and Laboratory Plasmas. Springer-Verlag, Berlin, Heidelberg, New York, pp. 1–403, 2002.
- Lipatov, A.S., Combi, M.R. Effects of kinetic processes in shaping Io's global plasma environment: a 3D hybrid model. *ICARUS* 180 (2), 412–427, 2006.
- Lipatov, A.S., Motschmann, U., Bagdonat, T. 3-D hybrid simulation of the interaction of the solar wind with a weak comet. *Planet. Space Sci.* 50, 403–411, 2002.
- Lipatov, A.S., Sauer, K., Baumgärtel, K. 2.5-D hybrid code simulation of the solar wind interaction with weak comets and related objects. *Adv. Space Res.* 20 (2), 279, 1997.
- Lipatov, A.S., Sittler, E.C., Hartle, R.E., Cooper, J.F., Simpson, D.G. Saturn's magnetosphere interaction with Titan for T9 encounter: 3D hybrid simulation and comparison with CAPS's observations. *Planet. Space Sci.*, submitted for publication.
- Lipatov, A.S., Zank, G.P., Pauls, H.L. The interaction of neutral interstellar H with the heliosphere: a 2.5-D particle-mesh boltzmann simulation. *J. Geophys. Res.* 103 (A12), 29679, 1998.
- Mankofsky, A., Sudan, R.N., Denavit, J. Hybrid simulation of ion beams in background plasma. *J. Comput. Phys.* 70, 89–116, 1987.
- Ma, Y.-J., Nagy, A.F., Toth, G., Cravens, T.E., Russell, C.T., Gombosi, T.I., Wahlund, J.-E., Crary, F.J., Coates, A.J., Bertucci, C.L., Neubauer, F.M. 3D global multi-species Hall-MHD simulation of the Cassini T9 flyby. *Geophys. Res. Lett.* 34, L24S10, doi:10.1029/2007GRL031627, 2007.
- Modolo, R., Chanteur, G.M., Wahlund, J.-E., Canu, P., Kurth, W.S., Gurnett, D., Matthews, A.P., Bertucci, C. Plasma environment in the wake of Titan from hybrid simulation: a case study. *Geophys. Res. Lett.* 34, L24S07, doi:10.1029/2007GL030489, 2007a.
- Modolo, R., Wahlund, J.-E., Boström, R., Canu, P., Kurth, W.S., Gurnett, D., Lewis, G.R., Coates, A.J. Far plasma wake of Titan from RPWS observations: a case study. *Geophys. Res. Lett.* 34, L24S04, doi:10.1029/2007GL030482, 2007b.
- Modolo, R., Chanteur, G.M. A global hybrid model for Titan's interaction with the Kronian plasma: application to the Cassini Ta flyby. *J. Geophys. Res.* 113, A01310, doi:10.1029/2007JA012453, 2008.
- Nagy, A.F., Liu, Y., Hansen, K.C., Kabin, K., Gombosi, T.I., Combi, M.R., DeZeeuw, D.L., Powell, K.G., Kliore, A.J. The interaction between the magnetosphere of Saturn and Titan's ionosphere. *J. Geophys. Res.* 106, 6151–6160, 2001.
- Sauer, K., Bogdanov, A., Baumgärtel, K., Dubinin, E. Plasma environment of comet Wirtanen during its low-activity stage. *Planet. Space Sci.* 44 (7), 715–729, 1996.
- Sauer, K., Lipatov, A.S., Baumgärtel, K., Dubinin, E. Solar wind-pluto interaction revised. *Adv. Space Res.* 20 (2), 295, 1997.
- Sillanpää, I., Kallio, E., Janhunen, P., Schmidt, W., Mursula, K., Vilpola, J., Tanskanen, P. Hybrid simulation study of ion escape at Titan for different orbital positions. *Adv. Space Res.* 28, 799–805, 2006.
- Simon, S., Kleindienst, G., Boesswetter, A., Bagdonat, T., Motschmann, U., Glassmeier, K.-H., Schüle, J., Bertucci, C., Dougherty, M. Hybrid simulation of Titan's magnetic field signature during the Cassini T9 flyby. *Geophys. Res. Lett.* 34, L24S08, doi:10.1029/2007GLO29967, 2007.
- Sittler, E.C., Hartle, R.E., Bertucci, C., Coates, A., Cravens, T., Dandouras, I., Shemansky, D. Energy deposition processes in Titan's Upper atmosphere and its induced magnetosphere, in: Brown, R.H., Lebreton, J.P., Waite, J.H. (Eds.), *Titan from Cassini-Huygens*. Springer, Dordrecht, Heidelberg, London, New York, pp. 393–455, 2009.
- Sittler, E.C., Hartle, R.E., Johnson, R.E., Cooper, J.F., Lipatov, A.S., Bertucci, C., Coates, A.J., Szego, K., Shappirio, M., Simpson, D.G., Wahlund, J.-E. Saturn's magnetospheric interaction with Titan as defined by Cassini encounters T9 and T18: new results. *Planet. Space Sci.* 58, 327–350, 2010.
- Sittler, E.C., Hartle, R.E., Lipatov, A.S., Cooper, J.F., Bertucci, C., Coates, A.J., Arridge, C., Szego, K., Johnson, R.E., Shappirio, M., Simpson, D.G., Tokar, R., Young, D.T. Saturn's magnetosphere and properties of upstream flow at Titan: preliminary results. *Planet. Space Sci.*, submitted for publication.
- Sittler Jr., E.C., Hartle, R.E., Vinäs, A.F., Johnson, R.E., Smith, H.T., Mueller-Wodarg, I. Titan interaction with Saturn's magnetosphere: Voyager 1 results revisited. *J. Geophys. Res.* 110, A09302, 1253, doi:10.1029/2004JA010759, 2005.
- Winske, D., Wu, C.S., Li, Y.Y., Mou, Z.Z., Guo, S.Y. Coupling of newborn ions to the solar wind by electromagnetic instabilities and their interaction with the bow shock. *J. Geophys. Res.* 90, 2713–2726, 1985.
- Yelle, R.V., Borggren, N., de la Haye, V., Kasprzak, W.T., Niemann, H.B., Müller-Wodarg, I., Waite Jr., J.H. The vertical structure of Titan's upper atmosphere from Cassini Ion Neutral Mass Spectrometer measurements. *Icarus* 182, 567–576, 2006.